Adsorption of Myoglobin to Cu(II)-IDA and Ni(II)-IDA Functionalized Langmuir Monolayers: Study of the Protein Layer Structure during the Adsorption Process by Neutron and X-Ray Reflectivity

M. S. Kent,* H. Yim, and D. Y. Sasaki

Sandia National Laboratories, Albuquerque, New Mexico 87185

Sushil Satija and Young-Soo Seo

NIST Center for Neutron Research, National Institutes of Standards and Technology, Gaithersburg, Maryland 20899

J. Majewski

Los Alamos Neutron Science Center, LANSCE-12, Los Alamos National Laboratory, Los Alamos, New Mexico 87545

Received October 18, 2004. In Final Form: April 26, 2005

The structure and orientation of adsorbed myoglobin as directed by metal−histidine complexation at the liquid−film interface was studied as a function of time using neutron and X-ray reflectivity (NR and XR, respectively). In this system, adsorption is due to the interaction between iminodiacetate (IDA)-chelated divalent metal ions Ni(II) and Cu(II) and histidine moieties at the outer surface of the protein. Adsorption was examined under conditions of constant area per lipid molecule at an initial pressure of 40 mN/m. Adsorption occurred over a time period of about 15 h, allowing detailed characterization of the layer structure throughout the process. The layer thickness and the in-plane averaged segment volume fraction were obtained at roughly 40 min intervals by NR. The binding constant of histidine with Cu(II)-IDA is known to be about four times greater than that of histidine with Ni(II)-IDA. The difference in interaction energy led to significant differences in the structure of the adsorbed layer. For Cu(II)-IDA, the thickness of the adsorbed layer at low protein coverage was ≤20 Å and the thickness increased almost linearly with increasing coverage to 42 Å. For Ni(II)-IDA, the thickness at low coverage was ∼ 38 Å and increased gradually with coverage to 47 Å. The in-plane averaged segment volume fraction of the adsorbed layer independently confirmed a thinner layer at low coverage for Cu(II)-IDA. These structural differences at the early stages are discussed in terms of either different preferred orientations for isolated chains in the two cases or more extensive conformational changes upon adsorption in the case of Cu(II)-IDA. Subphase dilution experiments provided additional insight, indicating that the adsorbed layer was not in equilibrium with the bulk solution even at low coverages for both IDA-chelated metal ions. We conclude that the weight of the evidence favors the interpretation based on more extensive conformational changes upon adsorption to Cu(II)-IDA.

I. Introduction

Metal ion affinity is commonly used for targeted adsorption of proteins via chelated metal-ion complex formation.[1−3] This method utilizes coordination interactions between metal ions and naturally occurring histidine units, genetically engineered metal-ion binding sites, or polyhistidine units (His tags) inserted at either the N or C terminus of proteins. This versatile method provides a strategy for selective adsorption of proteins in proteomics studies[4−6] for orienting proteins at engineered interfaces for biofunctionalization[7−9] and for 2-D crystallization of proteins.[10−12] Metal-ion affinity columns are used for purification and concentration of His-tagged fusion proteins, as well as many native and recombinant proteins. Histidine units bind to chelated divalent metal ions in the unprotonated state, and then the adsorbed proteins can be eluted by either lowering the pH or introducing a high concentration of free imidazole. This method can be used to separate proteins with different numbers of surface-exposed histidines or even proteins with the same number but different spatial distributions or local environments

(1) Arnold, F. H. *Biotechnology* **1991**, *9*, 151.
(2) Jones, C.; Patel, A.; Griffin, S.; Martin, J.; Young, P.; O'Donnell, K.; Silverman, C.; Porter, T.; Chaiken, I. *J. Chromatogr. A* **1995**, *707*, 3.
(3) Ueda E. K. M.; Gout, P. W.; Morganti, L. *J. Chromatogr. A* **2003**, *1*, 1.
(4) Ren, D.; Penner, N. A.; Slentz, B. E.; Mirzaei, H.; Regnier, F. *J. Proteome Res.* **2003**, *2*, 321.
(5) Slentz, B. E.; Penner, N. A.; Regnier, F. E. *J. Chromatogr. A* **2003**, *984*, 97.
(6) Wang, S.; Zhang, X.; Regnier, F. E. *J. Chromatogr. A* **2002**, *949*, 153.
(7) Dietrich, C.; Schmitt, L.; Tampé, R. *Proc. Natl. Acad. Sci. U.S.A.* **1995**, *92*, 9014.
(8) Dietrich, C.; Boscheinen, O.; Sharf, K. D.; Schmitt, L.; Tampé, R. *Biochemistry* **1996**, *35*, 1100.
(9) Celia, H.; Wilson-Kubalek, E.; Milligan, R. A.; Teyton, L. *Proc. Natl. Acad. Sci. U.S.A.* **1999**, *96*, 5634.
(10) Haas, H.; Brezesinski, G.; Mohwald, H. *Biophys. J.* **1995**, *68*, 312−314.
(11) Lenne, P. F.; Berge, B.; Renault, A.; Zakri, C.; Venien-Bryan, C.; Courty, S.; Balavoine, F.; Bergsma-Schutter, W.; Brisson, A.; Grubel, G.; Boudet, N.; Konovalov, O.; Legrand, J. F. *Biophys. J.* **2000**, *79*, 496−500.
(12) Courty, S.; Lebeau, L.; Martel, L.; Lenne, P. F.; Balavoine, F.; Dischert, W.; Konovalov, O.; Mioskowski, C.; Legrand, J. F.; Venien-Bryan, C. *Langmiur* **2002**, *18*, 9502.

10.1021/la047433q CCC: $30.25
Published on Web 06/18/2005

(pK_a and steric considerations).[1,13] The use of metal ion coordination to target the adsorption of proteins to lipid membranes has also received much attention.[1,7,8,10,12,14−22] Mixtures of metal-chelating lipids with other lipids are being investigated for protein detection schemes, as protein adsorption can lead to in-plane rearrangements of the lipids detectable by fluorescence techniques.[15,16]

Understanding the protein−membrane interaction and the dynamics of the adsorption process in greater detail will benefit many important applications. For example, genetic engineering of metal affinity sites for targeted adsorption of peptides or proteins requires optimizing the number and placement of histidine residues to tune the interaction strength and/or achieve a desired orientation. One example is the localization of antibodies to substrates in biosensors in an orientation that exposes the binding site(s). Many applications require that the native state of the protein be retained throughout the process. The conditions for which protein structure remains unaltered upon adsorption are not yet fully understood. Furthermore, many applications require release of proteins following binding. Selective release may be desired when more than one type of protein adsorbs. Selectivity, which is best achieved with weaker binding interactions, must be balanced against low retention. A deeper understanding of the kinetic and energetic factors impacting desorption will lead to better optimization of such systems. Purification of proteins by metal affinity chromotagraphy typically requires the use of His tags. In such cases, proteins with naturally occurring surface-exposed histidines may adsorb to metal affinity columns as well, acting as contaminants. In that case, it is desirable to design surfaces and solution conditions such that only His-tagged proteins adsorb strongly or the desired proteins can be selectively released by specific washing conditions or reagents.[23] In some cases, the purification of proteins with naturally occurring surface-exposed histidine residues is desired.[24] For all these applications, it is important to know if the native structure is retained and how to achieve selective adsorption or desorption and control over orientation.

Analyses of protein adsorption have involved both thermodynamic (equilibrium adsorption isotherms) and kinetic (modeling adsorption and desorption rates) approaches. The latter approach is used when attainment of equilibrium is in doubt. This occurs because the sum of the interactions with the substrate may greatly exceed kT, interactions among adsorbed proteins may stabilize the molecules against desorption,[25−29] and conformational changes may occur upon adsorption.[26,27,30−35] Unfolding increases entropy and allows internal regions of the protein to form additional contacts with sites on the surface. The tendency of some proteins to denature upon adsorption to (typically hydrophobic) surfaces while others do not has led to the terminology of "hard" and "soft" proteins. Myoglobin is considered a "soft" protein, whereas, for example, the more structurally stable lysozyme is considered a "hard" protein.[31] The extent of denaturation on solid surfaces can be probed by circular dichroism,[36−40] IR spectroscopy,[33,41,42] neutron reflection,[43] and AFM.[44−51] At the liquid−air interface, IR spectroscopy has been used.[52] In addition, polarized fluorescence measurements provide indirect insight via the average value and distribution of the tilt angle for porphyrin-containing proteins.[53,54]

Resolving various thermodynamic and kinetic effects can often be very difficult.[43,55−62] Studies involving the adsorption of lysozyme provide a good example. One group

(13) Hemdan, E. S.; Zhao, Y. J.; Sulkowski, E.; Porath, J. *Proc. Natl. Acad. Sci. U.S.A.* **1989**, *86*, 1811.
(14) Venien-Bryan, C.; Lenne, P. F.; Zakri, C.; Renault, A.; Brisson, A.; Legrand, J. F.; Berge B. *Biophys. J.* **1998**, *74*, 2649.
(15) Maloney, K. M.; Shnek, D. R.; Sasaki, D. Y.; Arnold, F. H. *Chem. Biol.* **1996**, *3*, 185.
(16) Pack, D. W.; Ng, K.; Maloney, K. M.; Arnold; F. H. *Supramol. Sci.* **1997**, *4*, 3.
(17) Frey, W.; William R. Schief, J.; Pack, D. W.; Chen, C.-T.; Chilkoti, A.; Stayton, P.; Vogel, V.; Arnold, F. H. *Proc. Natl. Acad. Sci. U.S.A.* **1996**, *93*, 4937.
(18) Shnek, D. R.; Pack, D. W.; Sasaki, D. Y.; Arnold, F. H. *Langmuir* **1994**, *10*, 2382−2388.
(19) Mallik, S.; Johnson, R. D.; Arnold, F. H. *J. Am. Chem. Soc.* **1994**, *116*, 8902.
(20) Ng, K.; Pack, D. W.; Sasaki, D. Y.; Arnold, F. H. *Langmuir* **1995**, *11*, 4048.
(21) Bischler, N.; Balavoine, F.; Milkereit, P.; Tschochner, H.; Mioskowski, C.; Schultz, P. *Biophys. J.* **1998**, *74*, 1522−1532.
(22) Rädler, U.; Mack, J.; Persike, N.; Jung, G.; Tampé, R. *Biophys. J.* **2000**, *79*, 3144.
(23) Westra, D. F.; Welling, G. W.; Koedijk, D. G. A. M.; Scheffer, A. J.; The, T. H.; Welling-Wester, S. *J. Chromatogr. B* **2001**, *760*, 129.
(24) Chaga, G.; Hopp, J.; Nelson, P. *Biotechnol. Appl. Biochem.* **1999**, *29*, 19.
(25) Ramsden, J. J.; Bachmanova, G. I.; Archakov, A. I. *Phys. Rev. E* **1994**, *50*, 5072.
(26) Green, R. J.; Hopkinson, I,; Jones, R. A. L. *Langmuir* **1999**, *15*, 5102.
(27) Adams, S.; Higgins, A. M.; Jones, R. A. L. *Langmuir* **2002**, *18*, 4854.
(28) Ball, A.; Jones. R. A. L. *Langmuir* **1995**, *11*, 3542.
(29) Ho, C. H.; Britt, D. W.; Hlady, V. *J. Mol. Recognit.* **1996**, *9*, 444.
(30) Norde, W. *Adv. Colloid Interface Sci.* **1986**, *25*, 267.
(31) Arai, T.; Norde, W. *Colloids Surf.* **1990**, *51*, 1.
(32) Arai, T.; Norde, W. *Colloids Surf.* **1990**, *51*, 17.
(33) Buijs, J.; Norde, W.; Lichtenbelt, J. W. Th. *Langmuir* **1996**, *12*, 1605.
(34) Schmidt, C. F.; Zimmermann, R. M.; Gaub, H. E. *Biophys. J.* **1990**, *57*, 577.
(35) Sharp, J. S.; Forrest, J. A.; Jones, R. A. L. *Biochemistry* **2002**, *41*, 15810.
(36) Kondo, A.; Fukuda, H. *J. Colloid Interface Sci.* **1998**, *198*, 34.
(37) Billsten, P.; Wahlgren, M.; Arnebrant, T.; McGuire, J.; Elwing, H. *J. Colloid Interface Sci.* **1995**, *175*, 77.
(38) Kondo, A.; Urabe, T. *J. Colloid Interface Sci.* **1995**, *174*, 191.
(39) Edminston, P. L.; Lee, J. E.; Cheng, S.-S.; Saavedra, S. S. *J. Am. Chem. Soc.* **1997**, *119*, 560.
(40) Zougrana, T.; Findenegg, G. H.; Norde, W. *J. Colloid Interface Sci.* **1997**, 190, 437.
(41) Bentalab, A.; Abele, A.; Haikel, Y.; Schaaf, P.; Voegel, J. C. *Langmuir* **1998**, *14*, 6493.
(42) Cheng, S.-S.; Chittur, K. K.; Sukenik, C. N.'; Culp, L. A.; Lewandowski, K. *J. Colloid Interface Sci.* **1994**, *162*, 135.
(43) Lu, J. R.; Su, T. J.; Thirtle, P. N.; Thomas, R. K.; Rennie, A. R.; Cubitt, R. *J. Colloid Interface Sci.* **1998**, *206*, 212.
(44) Cullen, D. C.; Lowe, C. R. *J. Colloid Interface Sci.* **1994**, *166*, 102.
(45) Sagvolden, G.; Giaver, I.; Feder, J. *Langmuir* **1998**, *14*, 5984.
(46) Lin, J. N.; Drake, B.; Lea, A. S.; Hansma, P. K.; Andrade, J. D. *Langmuir* **1990**, *6*, 509.
(47) Mcmaster, T.; Miles, M. J.; Shewry, P. R.; Tatham, A. S. *Langmuir* **2000**, *16*, 1463.
(48) Ta, T. C.; Sykes, M. T.; McDermott, M. T. *Langmuir* **1998**, *14*, 2435.
(49) Kidoaki, S.; Matsuda, T. *Langmuir* **1999**, *15*, 7639.
(50) Hemmerle, J.; Altmann, S. M.; Maaloum, M.; Horber, J. K. H.; Heinrich, L.; Voegel, J.-C.; Schaaf, P. *Proc. Natl. Acad. Sci. U.S.A.* **1999**, *96*, 6705.
(51) Sheller, N. B. Petrash, S.; Foster, M. D. *Langmuir* **1998**, *14*, 4535.
(52) Chen, H.; Hsu, S. L.; Tirrell, D. A. *Langmuir* **1997**, *13*, 4775.
(53) Tronin, A.; Strzalka, J.; Chen, X.; Dutton, P. L.; Blasie, J. K. *Langmuir* **2000**, *16*, 9878.
(54) Tronin, A.; Strzalka, J.; Chen, X.; Dutton, P. L.; Ocko, B. M.; Blasie, J. K. *Langmuir* **2001**, *17*, 3061.
(55) Fragneto, G.; Lu, J. R.; McDermott, D. C.; Thomas, R. K.; Rennie, A. R.; Gallagher, P. D.; Satija, S. K. *Langmuir* **1996**, *12*, 477.
(56) Sigal, G. B.; Mrksich, M.; Whitesides, G. M. *J. Am. Chem. Soc.* **1998**, *120*, 3464.
(57) Wertz, C. F.; Santore, M. M. *Langmuir* **2002**, *18*, 1190.
(58) Yan, G.; Li, J.-T.; Huang, S.-C.; Caldwell, K. D. In *Proteins at interfaces II: fundamentals and Applications*; Brash, J. L., Horbett, T. A., Eds.; ACS Symposium 02; American Chemical Society: Washington, DC, 1995; p 256.
(59) Haynes, C.; Norde, W. *J. Colloid Interface Sci.* **1994**, *164*, 394.
(60) Lee, C. S.; Belfort, G. *Proc. Natl. Acad. Sci. U.S.A.* **1989**, *86*, 8392.
(61) Wertz, C. F.; Santore, M. M. *Langmuir* **1999**, *15*, 8884.
(62) Wertz, C. F.; Santore, M. M. *Langmuir* **2001**, *17*, 3006.

reported denaturation of lysozyme upon adsorption to hydrophobic self-assembled monolayers,[43] whereas another group reported that the native state was maintained.[56] More recently, a third group reported reversible adsorption in an end-on orientation followed by relaxation to a side-on orientation.[57] In another study, the adsorption of ribonuclease A to mica was explained in terms of thermodynamic equilibrium.[60] In that study, the activity of adsorbed ribonuclease A was observed to increase with increasing coverage. This was attributed to a reorientation phase transition with increasing coverage that made the binding site more accessible.

Metal-ion chelating systems have been analyzed largely in terms of equilibrium adsorption isotherms[63,64] despite the fact that strong irreversible (with respect to bulk concentration) association is essential for the efficiency of protein separation in immobilized metal affinity chromatography (IMAC). These systems indeed show some apparent signatures of equilibrium, including a strong dependence of adsorbed amount (Γ, determined at an arbitrarily specified time) on bulk protein concentration (c_p), especially a sharp increase in Γ at a critical bulk concentration (c_p^*), and a strong dependence of c_p^* on binding energy (metal ion). However, we show below that, for myoglobin adsorbing to a metal-ion chelating lipid loaded with either Cu(II) or Ni(II) ions, the adsorbed layer is not in equilibrium with the bulk even for low protein coverages. In light of this, c_p^* should be considered the bulk concentration at which the kinetics of adsorption are strongly accelerated. The question of equilibration at low coverage is pertinent to the interpretation of the structural data reported below since equilibration is inconsistent with denaturation.

We have begun a study of the structure of proteins adsorbed to membranes of metal-chelating lipids using grazing incidence neutron and X-ray techniques.[65] Neutron and X-ray reflectivity are used to determine the thickness and average segment volume fraction of the adsorbed layer. The thickness, combined with the known dimensions of the protein, enables the orientation to be inferred if no structural changes occur upon adsorption.[66] Grazing incidence X-ray diffraction is used to probe for ordering within the protein−lipid structure. Previously, we reported results on the adsorption of horse skeletal muscle myoglobin to a Langmuir monolayer composed entirely of 1,2-disterylglycero-3-triethyleneoxideiminodiacetatic acid (DSIDA).[65] This synthetic lipid has an iminodiacetate (IDA) headgroup for metal-ion chelation and two saturated aliphatic tails with 18 carbons each. IDA, a tridentate chelator widely used in metal affinity chromatography, binds Cu(II) with an affinity constant of 10^{11} M^{-1}.[67] This densely packed lipid monolayer provides a very high density of binding sites. In the previous work, the adsorbed layer structure after 12−15 h was compared for chelated Cu(II) and Ni(II) ions. The binding constant ($K = e^{-\Delta G/RT}$) of a single protein histidyl with Cu(II)-IDA at room temperature has been reported to be 4.5×10^3 M^{-1},[1] corresponding to a binding energy of $8.4kT$. This is very similar to the binding constant of low-molecular-weight histidine derivatives with Cu(II)-IDA at 25 °C (3.4×10^3 M^{-1} corresponding to 4.8 kcal/mol or $8.1kT$).[63,68] The binding constant of histidine with Ni(II)-IDA is roughly a factor of 4 lower than that for histidine with Cu(II)-IDA,[68,69] corresponding to a binding energy of about $6.8kT$ at 25 °C.

Myoglobin's native structure is known in great detail, and its interaction with Cu(II)-IDA complexes has been studied previously by other methods.[18,70] The mean charge is 0 at pH 7.3, where the present experiments were performed, so the effects of electrostatic interactions should be minimal. The dimensions calculated from the crystal structure are approximately 44 Å × 44 Å × 25 Å. Horse skeletal muscle myoglobin has 11 histidines of which five (His-36, His-48, His-81, His-113, and His-116) are on the outer exposed surface and are readily available to interact with the lipid film. Initial binding occurs only through surface-accessible histidines, as has been shown in a previous study involving A. limacine myoglobin,[13] which has no surface-accessible histidines. In that study, no retention of A. limacine myoglobin on an Cu(II)-IDA IMAC column was observed.

Our previous report focused only on results obtained at relatively long times (12−15 h) at fixed area per DSIDA molecule. At myoglobin concentrations below c_p^*, the adsorbed layer structures were quite different, with a substantially thinner layer observed in the case of Cu(II). For $c_p > c_p^*$, the thickness and segment concentrations of the layers were comparable for chelated Cu(II) and Ni(II) ions. Little change was observed in the crystalline packing of the lipid tails upon protein binding.

In this report, we present the time evolution of the protein layer during the adsorption process, again emphasizing differences that appear as a function of interaction strength (chelated metal ion). We show more detailed evidence of structural differences at low coverages for chelated Cu(II) and Ni(II) ions. We demonstrate that these differences are only a function of the areal density of adsorbed molecules, the same whether obtained for low bulk myoglobin concentrations at long times or at high bulk concentrations at short times. We will argue that the results point to more extensive conformational changes of myoglobin upon adsorption to Cu(II)-IDA than to Ni(II)-IDA.

II. Experimental Section

Materials. The synthesis of DSIDA has been described previously.[20] Myoglobin from horse skeletal muscle (>95% pure) and chicken egg white lysozyme were purchased from Sigma.[70] $CuCl_2$ (99.999%) and $NiCl_2$ (99.9%) were purchased from Aldrich. Phosphate buffer saline (PBS) solution (pH 7.3) was prepared by dissolving sodium hydrogenphosphate heptahydrate (8.16 g), sodium dihydrogenphosphate monohydrate (1.20 g), and sodium chloride (5.86 g) in 1 L of deionized water (Barnstead Nanopure, resistivity 18 MΩ). Stock solutions of myoglobin and lysozyme were prepared by dissolving each in 10 mL of the phosphoric acid buffer solution to a concentration of 2 mM. Stock solutions of $CuCl_2$ and $NiCl_2$ were prepared by dissolving the compounds in 10 mL of deionized water to give a concentration of 6.6 mM.

Methods. Neutron reflection was performed on the NG7 (NIST, http://ncnr.nist.gov/instruments/ng7refl) and SPEAR (Los Alamos, http://lansce.lanl.gov/lujan/instruments/spear/spear.htm) reflectometers. Complementary XR experiments were performed using the liquid surface spectrometer at the Advanced

(63) Todd, R. J.; Johnson, R. D.; Arnold, F. H. *J. Chromatogr. A* **1994**, *662*, 13.
(64) Johnson, R. D.; Arnold, F. H. *Biochem. Biophys. Acta* **1995**, *1247*, 293.
(65) Kent, M. S.; Yim, H.; Sasaki, D. Y.; Satija, S.; Majewski, J.; Gog. T. *Langmuir* **2004**, *20*, 2819.
(66) Su, T. J.; Green, R. J.; Wang, Y.; Murphy, E. F.; Lu, J. R.; Ivkov, R.; Satija, S. K. *Langmuir* **2000**, *16*, 4999.
(67) Martell, A. E.; Smith, P. M. *Critical Stability Constants*; Plenum Press: New York, 1974; Vol 6.
(68) Sinha, P. C.; Saxena, V. K.; Nigam, N. B.; Sriastava, M. N. *Ind. J. Chem.* **1989**, *28A*, 335.
(69) In ref 65, we stated that the affinity of histidine for Cu−IDA is 15 times that for Ni(II)-IDA. However, that is incorrect. The factor of 15 was cited by Arnold for imidazole with free Cu(II) and Ni(II),[1] not Cu(II) and Ni(II) bound to IDA.
(70) Wuenschall, G. E.; Wen, E.; Todd, R.; Shnek, D.; Arnold, F. H. *J. Chromatogr.* **1991**, *543*, 345.

Photon Source (CMC-CAT, Argonne National Laboratory) and an in-house X-ray reflectometer (Bruker) employing Cu K_α radiation at NIST. The techniques for preparing the monolayers and circulating the metal ions and myoglobin underneath the monolayer have been described previously.[65] For all the data reported below, the circulation pump was turned off after ~1 h to minimize vibrations during the reflectivity measurements. (Later measurements showed that reflectivity measurements are unaffected if the pump operates at low rates.) Subphase exchange was accomplished by simultaneously pumping the subphase out from one end of the trough into a reservoir and pumping from the reservoir into the subphase underneath the monolayer at the other end of the trough. Precise control of the two rates allowed the meniscus to be maintained.

Two approaches were used to collect reflectivity scans during the adsorption process. In one method (NG7 reflectometer, NIST), a fixed wavelength was selected and data were collected successively for a small number of angles in the range of momentum transfer ($q_z = 4\pi \sin\theta/\lambda$) from 0.02 to 0.10 Å^{-1}. About 40 min were required to collect data with adequate statistics over this q_z range. The second method (SPEAR reflectometer, LANSCE) used the time-of-flight approach. In this case, the angle was fixed and data were collected simultaneously for a range of wavelengths covering a range of q_z from 0.015 to 0.12 Å^{-1}. In this case, the data were collected for 1 h periods. In each case, at the end of the adsorption process, data were collected over a longer time period to obtain better statistics in the final state.

The reflectivity data were analyzed using a least-squares fitting procedure involving multilayer models.[71] Analysis of the NR data to obtain the characteristics of the protein layer required an accurate model for the lipid layer. This was determined from XR data, which was obtained over a much larger range of q_z. The model for the lipid layer and the change in the lipid layer upon protein adsorption were first determined from the XR data, and then this information was imposed in the fits to the NR data. The XR data for the metal ion-loaded DSIDA in absence of myoglobin required three slabs in the model profile. The electron density within the tail layer was constrained to be consistent with the known area per molecule of 40 Å^2 at 40 mN/m from the pressure−area isotherm[18] and the atomic composition of DSIDA. Since the XR data showed very little change in the lipid tail region upon adsorption of myoglobin and since protonated lipids were used which resulted in little contrast between the protein and the lipid headgroups in NR, when fitting the NR data, the parameters for the lipid layers (two in modeling NR data) were fixed to the values obtained in the absence of myoglobin. Thus, fitting of the NR data in the presence of myoglobin involved only three free parameters: the thickness, scattering length density (SLD), and roughness of the protein layer. The range of uncertainty in each fitted parameter was determined by fixing that parameter at various values and allowing the other parameters to vary in the fitting within physically reasonable limits. Upper and lower bounds were determined by the values that led to fits which were unacceptably poor as judged by an increase in χ^2 by a factor of 1.5 (1.5 is an arbitrary but very conservative value). The reported thicknesses were obtained by fitting a polynomial to a plot of χ^2 versus thickness and obtaining the minimum, as shown in the previous report.[65]

III. Results

Neutron Reflectivity. NR data as a function of time are shown in Figure 1a for adsorption of myoglobin at a 10 μM bulk concentration to Cu(II)-DSIDA monolayers. Reflectivity scans were performed at ~40 min intervals after injecting myoglobin into the subphase. Analogous data are shown in Figure 1b for adsorption of myoglobin from a 100 μM bulk concentration to Ni(II)-DSIDA monolayers. In that case, the reflectivity scans were performed at ~1 h intervals after addition of myoglobin.

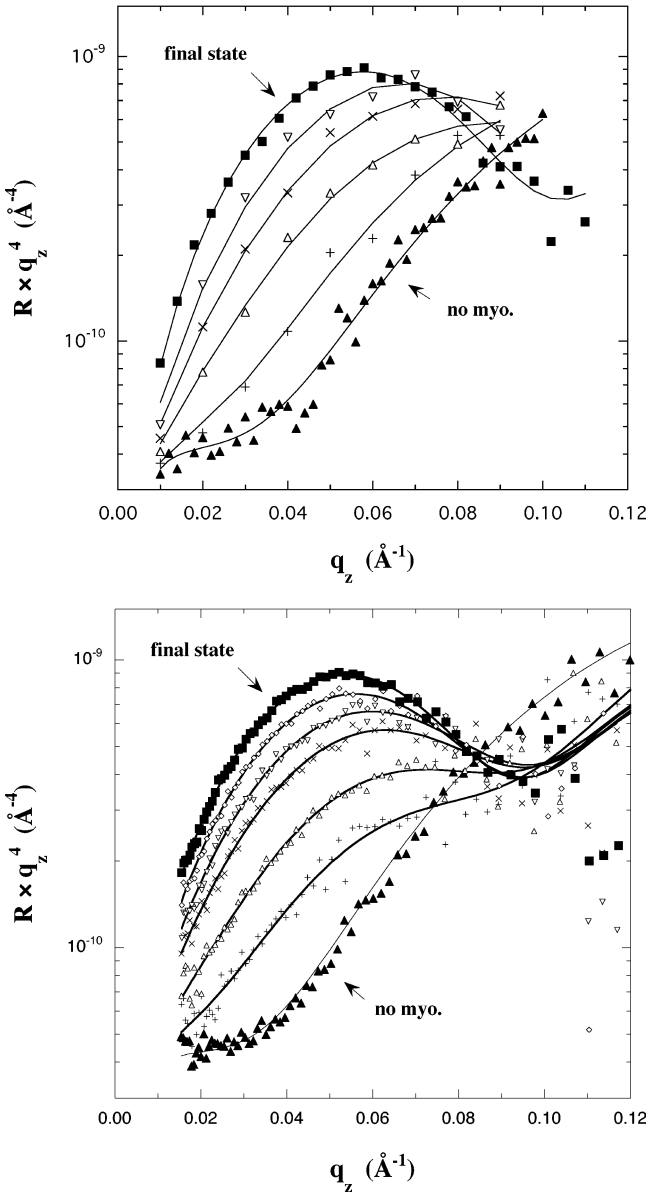

Figure 1. (a) Neutron reflectivity data for myoglobin adsorbing to Cu(II)-loaded DSIDA at a solution concentration of 10 μM. Data are shown prior to injecting myoglobin (▲) and for the following times after injecting myoglobin: 5.5 h (+), 7.5 (△), 9.0 (×), 11.0 (▽), and 15.9 h (■). (b) Neutron reflectivity data for myoglobin adsorbing to Ni(II)-loaded DSIDA at a solution concentration of 100 μM. Data are shown prior to injecting myoglobin (▲) and for the following times after injecting myoglobin: 1.1 (+), 1.9 (△), 3.6 (×), 5.3 (▽), 8.9 (◇), and 18.9 h (■).

Differences in the structure of the adsorbed layers at early times in the two cases are immediately evident in these data, as the curves at early times cross that for DSIDA-Ni(II) at q_z values less than 0.09 Å^{-1} whereas the curves obtained at short times remain well above that for DSIDA-Cu(II) over the same q_z range.

Adsorbed amounts were determined by integrating the profiles obtained from the fitting analysis. The adsorbed amount as a function of time for Cu(II)-DSIDA is shown in Figure 2a for bulk myoglobin concentrations of 10 (NR), 50 (NR), and 100 μM (XR). For the case of 10 μM myoglobin, data for longer times were obtained by XR. These data, shown in the inset, demonstrate that the adsorbed amount levels off after about 12−15 h for this case. The adsorbed amount as a function of time for myoglobin adsorbing to Ni(II)-DSIDA is shown in Figure 2b for bulk concentrations

(71) Certain trade names and company products are identified in order to specify adequately the experimental procedure. In no case does such identification imply recommendation or endorsement by the National Institute of Standards and Technology, nor does it imply that the products are necessarily the best for the purpose.

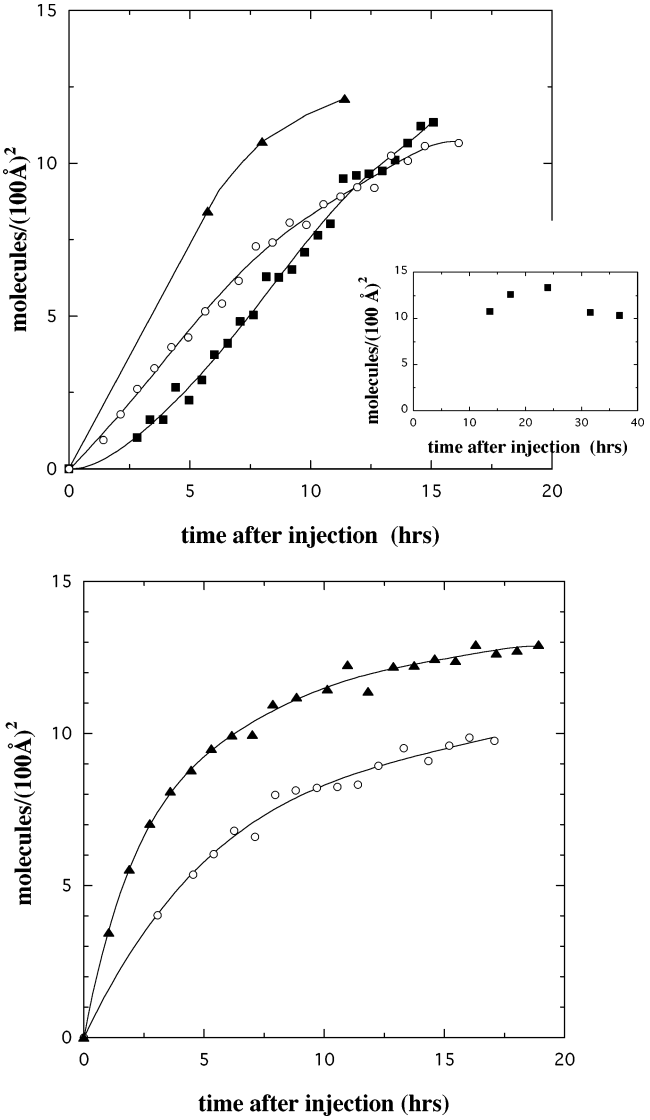

Figure 2. (a) Adsorbed amount as a function of time after injecting myoglobin for Cu(II)-loaded DSIDA and bulk myoglobin concentrations of 10 (■), 50 (○), and 100 μM (▲). The data for 10 and 50 μM were obtained by NR, and the data for 100 μM were obtained by XR. The inset shows data for 10 μM myoglobin at longer times obtained by XR. (b) Adsorbed amount as a function of time after injecting myoglobin for Ni(II)-loaded DSIDA and bulk myoglobin concentrations of 50 (○) and 100 μM (▲). Both sets were obtained by NR.

of 50 and 100 μM, both by NR. Both sets of data show that the initial rate of adsorption depends strongly on the bulk myoglobin concentration.

The adsorbed amounts obtained ~15 h after injection of myoglobin are plotted versus bulk concentration in Figure 3. Each curve shows a strong increase in adsorbed amount at a critical bulk concentration c_p*. For Cu(II)-DSIDA, this occurs at a concentration about a factor of 10 lower than for Ni(II)-DSIDA.[68] This is substantially larger than the factor of 4 difference in the binding constants of histidine with Cu(II)-IDA and Ni(II)-IDA. We show below that the systems are not in equilibrium even at low coverages, and therefore, binding constants for the protein cannot be accurately determined from these data by fitting to Langmuir or other equilibrium adsorption isotherms.[73] We were unable to obtain reflectivity data at higher myoglobin concentrations due to the difficulty of obtaining

(72) Russell, T. P. *Mater. Sci. Rep.* **1990**, *5*, 171.

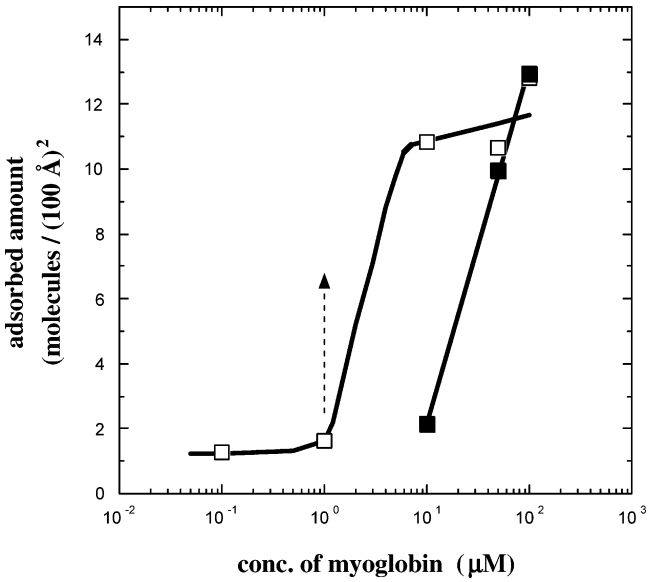

Figure 3. Adsorbed amount versus bulk myoglobin concentration for DSIDA loaded with Cu(II) (□) and Ni(II) (■). Adsorbed amounts were obtained from the reflectivity data collected at ~15 h after injection of myoglobin. The dashed line indicates the results for a run with $c_p < c_p$* that was followed for 48 h. In that case, adsorption did not plateau after 15 h but continue to gradually increase.

a sufficiently high subphase meniscus for the reflectivity measurement while avoiding spilling over the edges of the trough. In the case of adsorption to Cu(II)-IDA at a bulk concentration of 1 μM, in one experiment adsorption was followed for 48 h using XR. In that case, the adsorbed amount did not plateau at ~15 h but continued to increase gradually during the entire 48 h. The adsorbed amount was ~2 molecules/(100 Å)^2 at 12 h and increased to 7 molecules/(100 Å)^2 at 48 h. This experiment is depicted by the dashed line in Figure 3. Thus, we conclude that the data in Figure 3 do not represent equilibrium adsorption isotherms, but rather c_p* indicates the bulk concentration at which the kinetics of adsorption are strongly accelerated. We do not understand the mechanism for this at present.

To obtain data at short time intervals relative to the time scale of adsorption, the reflectivity scans were limited to the range of q_z up to 0.l0 (NG7) or 0.12 Å^{-1} (SPEAR). However, this range is sufficient to give an accurate measurement of the thickness and segment volume fraction within the layer, providing insight into the evolution of the layer structure during the adsorption process. The thickness versus adsorbed amount in each case is given in Figure 4a. The open symbols indicate data obtained as a function of time for bulk myoglobin concentrations of 10 and 50 μM in the case of Cu(II) and 50 and 100 μM in the case of Ni(II). The filled symbols indicate data obtained at ~15 h for various bulk myoglobin concentrations, including 0.1 and 1 μM in the case of Cu(II) and 10 μM in the case of Ni(II). Analogous data for the in-plane averaged amino acid volume fraction are shown in Figure 4b. The thickness and average segment volume fraction are a function only of the number of adsorbed molecules per area. For a given areal density of adsorbed protein, the same thickness and segment volume fraction are obtained at long times and low bulk concentrations

(73) Norde, W.; Haynes, C. A. In *Proteins at Interfaces II: Fundamentals and Applications*; Brash, J. L., Horobett, T. A. Eds.; ACS Symposium 602; American Chemical Society: Washington, DC, 1995; p 26.

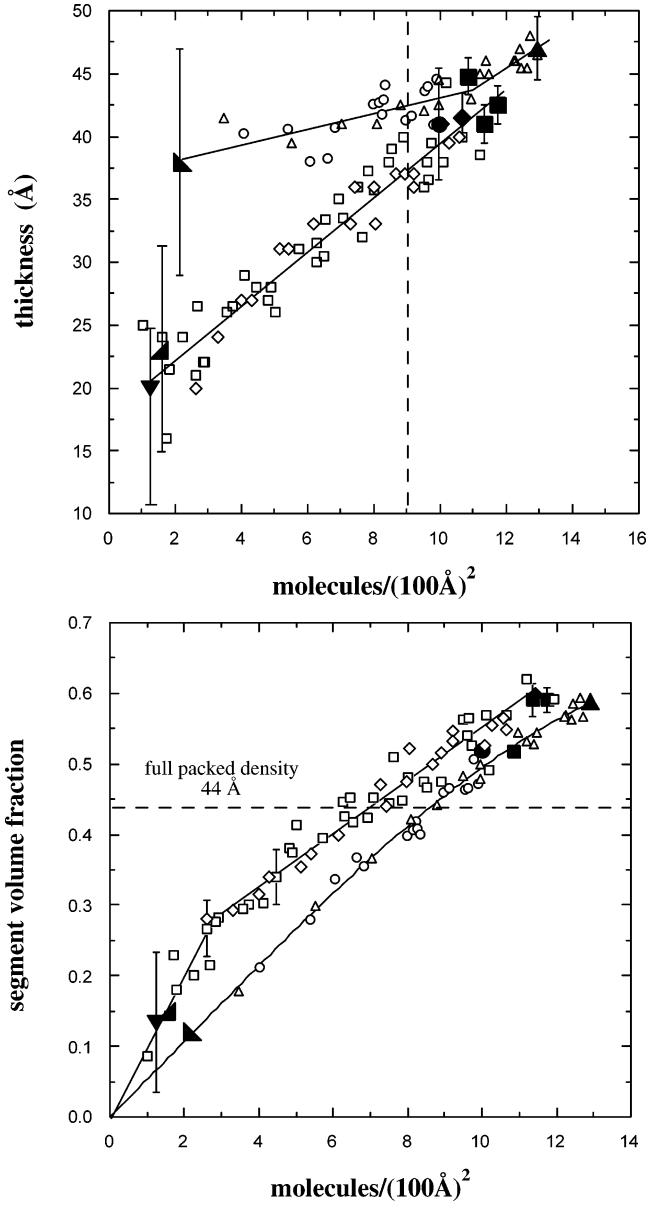

Figure 4. (a) Thickness of the adsorbed layer of myoglobin versus the adsorbed amount. Filled symbols indicate data obtained at ~15 h after injection. Open symbols indicate data obtained as a function of time. Results are shown for adsorption to Cu(II)-loaded DSIDA for bulk myoglobin concentrations of 0.1 (▼), 1 (◭), 10 (■,□), and 50 μM (◆, ◇), and for adsorption to Ni(II)-loaded DSIDA for bulk myoglobin concentrations at 10 (◭), 50 (●, ○), and 100 μM (▲, △). The dashed line indicates the adsorbed amount calculated from the crystallographic data assuming a dense packed monolayer with thickness of 44 Å. (b) Average amino acid volume fraction in the layer versus the adsorbed amount. The symbols are the same as in (a).

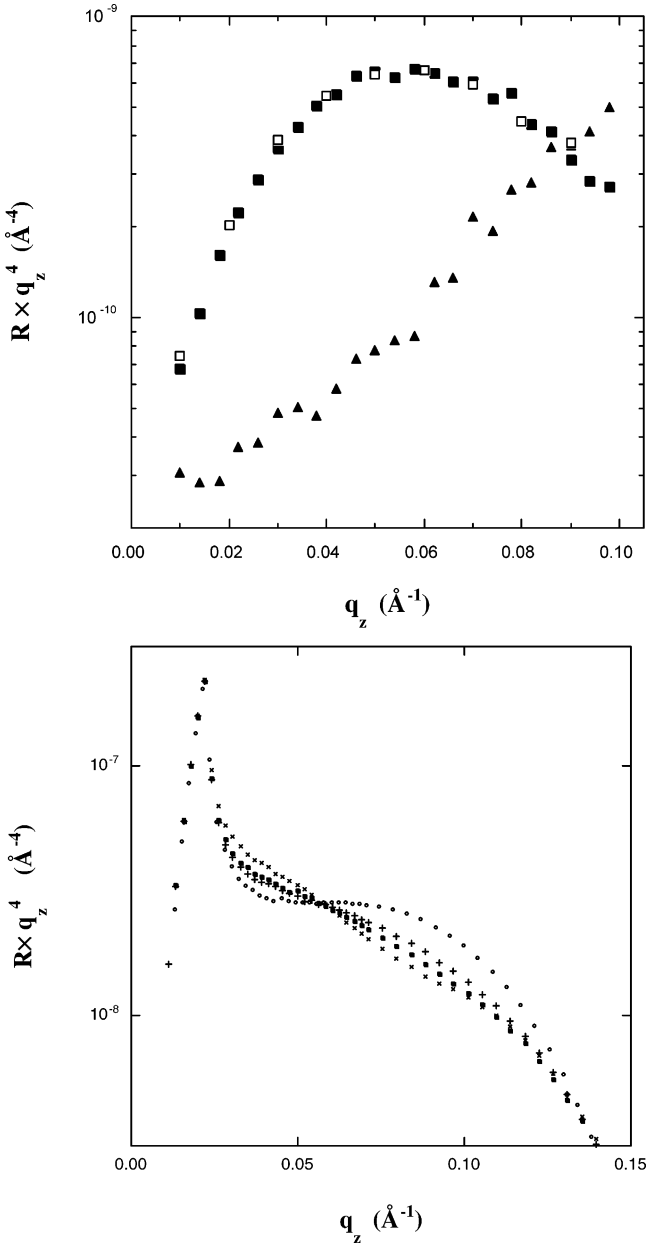

Figure 5. (a) Neutron reflectivity data for myoglobin adsorbing to Cu(II)-loaded DSIDA at a bulk myoglobin concentration of 50 μM. Data are shown prior to injecting myoglobin (▲), 16 h after injecting myoglobin (■), and 8 h after exchanging the 200 mL subphase with two liters of pure buffer to yield a final concentration of 1.4 μM (□). (b) X-ray reflectivity data for myoglobin adsorbing to Ni(II)-loaded DSIDA at a bulk myoglobin concentration of 60 μM. Data are shown prior to injecting myoglobin (○), 9 h after injecting myoglobin and immediately prior to exchanging the subphase (+), immediately after exchanging the 200 mL subphase with one liter of pure buffer to yield a final concentration of 10 μM (■), and 7 h after exchanging the subphase (×).

or at short times and high bulk concentrations. The maximum adsorbed amount corresponds to ~13 molecules/(100 Å)^2 or 3.7 mg/m^2.

Finally, to test the tenacity and reversibility of the adsorbed layer, in several cases, the subphase was diluted after the monolayer had formed. For the case of an initial bulk myoglobin concentration of 50 μM and chelated Cu(II) ions, adsorption was followed for 16 h, at which point the adsorbed amount approached an asymptotic value. Then, the subphase in the 200 mL trough was exchanged and equilibrated twice with a liter of pure buffer solution. This resulted in a final bulk myoglobin concentration of 1.4 μM. The entire process took about 2 h. Following exchange, the reflectivity was monitored for a period of 8 h. The data are shown in Figure 5a. No change in the reflectivity was observed over this time period, indicating that the adsorbed layer is irreversible on this time scale. In another experiment, this time using XR, adsorption of myoglobin at 60 μM (above c_p*) to Ni(II)-IDA was followed until only a fraction of the ultimate adsorbed amount was attained (9 h after injection). Then, the subphase was diluted with a liter of pure buffer solution, yielding a final concentration of ~10 μM (below c_p*). Beginning immediately after exchange, the reflectivity was followed

for a period of 7 h. The data are shown in Figure 5b. Surprisingly, instead of decreasing after subphase dilution, the adsorbed amount increased substantially to a final coverage that far exceeded the value obtained over the same time period when adsorption proceeded from the start with a bulk subphase concentration of 10 μM. Several further experiments were performed in which the subphase was exchanged at even earlier stages in the adsorption process, down to only 2 h after injection. Following subphase exchange, all showed significant adsorption beyond that expected in the same time period had the experiment proceeded from the start with 10 μM myoglobin. The fact that adsorption occurs after subphase exchange demonstrates that the adsorbed layer is not in equilibrium with the bulk. In addition, the enhanced rate of adsorption after exchange, relative to that had the experiment proceeded from the start with a bulk concentration of 10 μM, suggests that adsorbed myoglobin molecules somehow facilitate the adsorption of additional protein molecules.

Surface Pressure. The increase in surface pressure as a function of time after injecting myoglobin for the case of adsorption to Cu-loaded DSIDA at 40 Å^2 per molecule is shown in Figure 6a. Data are shown for 10 and 50 μM myoglobin. Analogous data for adsorption to Ni-loaded DSIDA for 50 and 100 μM myoglobin are shown in Figure 6b. It was found to be important to use Teflon tubing to eliminate contamination. For both bound metal ions, the pressure increased more rapidly with higher bulk concentration of myoglobin. More importantly, the pressure increase observed for Ni(II)-loaded DSIDA was much lower than that for Cu(II)-loaded DSIDA despite the fact that the final adsorbed amount was comparable in the two cases after ~15 h (Figure 4). This suggests that more insertion of myoglobin segments occurs upon adsorption to Cu(II)-DSIDA than upon adsorption to Ni(II)-loaded DSIDA.

IV. Discussion

We begin by considering the question of equilibrium. This bears on the interpretation of the structural data in that equilibration at low coverages would argue strongly against substantial conformational changes occurring upon adsorption. However, the subphase exchange experiments unequivocally demonstrate that the system is not at equilibrium for low coverages for both Ni(II)-DSIDA and Cu(II)-DSIDA.[74] Furthermore, while there is a strong dependence of the coverage measured after ~15 h on bulk concentration (Figure 3) when followed for an even longer time period, the coverage for $c_p < c_p^*$ does not plateau at 15 h but continues to gradually increase. This further demonstrates that the adsorbed layer is not in equilibrium with the bulk at low coverages. Thus, adsorption appears to be controlled by nonequilibrium processes, the kinetics of which depend strongly upon bulk protein concentration and also on the nature of the chelated metal ion.

The very slow time scale for adsorption is striking. While the initial adsorption rate depends strongly on bulk protein concentration, the time scales are far longer than can be accounted for by the diffusion coefficient of the protein in solution. For comparison, Wertz and Santore reported adsorption plateaus obtained in less than 1 h for BSA adsorption to C16 self-assembled monolayers from a bulk concentration of 0.01 mg/mL.[61] Likewise, Lin and Hlady reported adsorption plateaus occurring in less than 1 min for HSA adsorption to C18 self-assembled monolayers from a bulk concentration of 0.042 mg/mL.[75] In the present experiments, 10 μM myoglobin corresponds to ~0.17 mg/mL, yet the adsorption plateaus only after ~15 h. Thus, the dependence of the initial adsorption rate on bulk concentration must arise from a process other than diffusion. This underlines an important difference between protein adsorption driven by specific versus nonspecific interactions. We suggest that, for binding to occur in the present system, the protein must approach a M(II)-IDA binding site with a surface-accessible histidine in a precise orientation. This could explain both the dependence of the initial adsorption rate on bulk protein concentration and the very slow time scale of the adsorption process

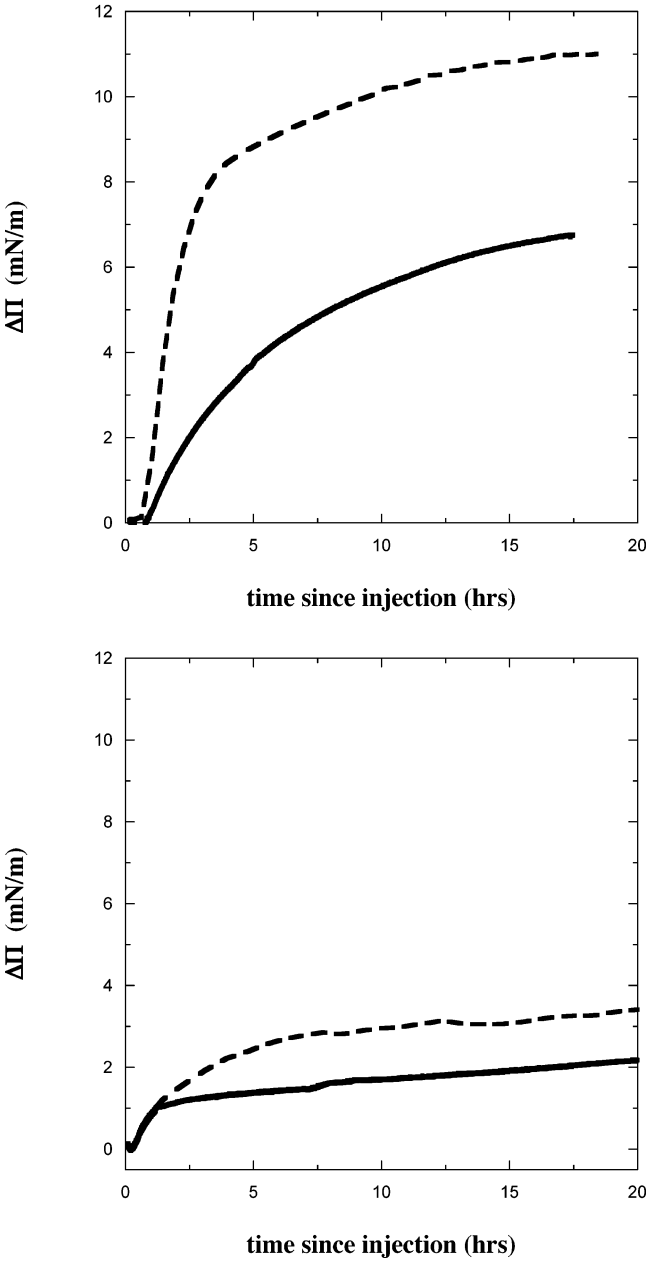

Figure 6. (a) Change in surface pressure with time after injecting myoglobin for adsorption to Cu(II)-loaded DSIDA. The two curves indicate bulk myoglobin concentrations of 10 (solid line) and 50 μM (dashed line). (b) Analogous data for adsorption to Ni(II)-loaded DSIDA. The two curves indicate bulk myoglobin concentrations of 50 (solid line) and 100 μM (dashed line).

(74) Lin, Y.-S., Hlady, V. *Colloids Surf., B* **1994**, *2*, 481.

(75) In ref 65, the term quasi-equilibrium was used to describe the state after ~12−15 h. The data in Figure 5 show that the systems are not in equilibrium, so the use of that term is incorrect.

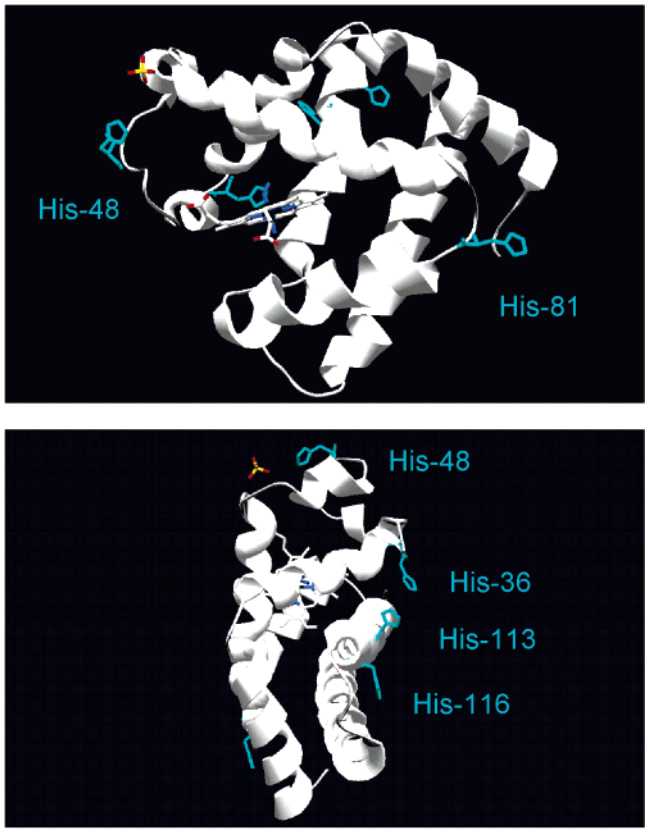

Figure 7. The structure of horse myoglobin with the five surface-exposed histidines highlighted.

compared to adsorption by nonspecific hydrophobic interactions. The capture cross-section is apparently greater for Cu(II)-IDA than for Ni(II)-IDA. Another possibility is a process analogous to Michaelis−Menten kinetics, such that the protein and chelated metal ions are in equilibrium with a protein/bound metal ion complex which may slowly convert to a state that is irreversible.

Recently, a strong dependence of ultimate adsorbed amount on bulk protein concentration for albumin and fibrinogen adsorbing onto hydrophobic surfaces was shown to be due to a kinetic effect rather than equilibration with the bulk.[61,62] In that study, kinetic data and variations in ultimate adsorbed amounts were interpreted as indicating denaturation and spreading on the surface on a time scale that was comparable with that of diffusion of protein to the surface. Higher bulk concentrations led to faster adsorption, restricted spreading, and thus a different final structure in the layer with a higher adsorbed amount. The present method allows a direct test of that mechanism by examining the structure of the layer at the same coverage but for differing bulk concentrations. As the data in Figure 4 show, this explanation is not valid for the present system since the same layer structure results at low coverages regardless of the bulk concentration. Furthermore, as mentioned above, the time scale is far too long to be explained by diffusion.

Next, we focus on the differences in the structural data for myoglobin adsorbing to Cu(II) and Ni(II) shown in Figure 4. We begin with a description of the distribution of the surface accessible histidines. His-48 and His-81 appear to be the most accessible. As shown in Figure 7, they are at opposite ends of one of the long dimensions of the protein and are located such that, if either one binds, no other histidine is able to bind to the surface in the absence of conformational changes. Binding by His-48 or His-81 would lead to an end-on orientation. His-113 and His-116 are located on an α-helix on one side of this disk-shaped protein (Figure 7).[76] In the native state, His-113 or His-116 could bind to the flat M(II)-IDA-functionalized surface along with His-36 in a side-on orientation. Aside from this possibility, significant conformational changes would be required to enable multiple histidines to bind.

The ∼38 Å thickness at low coverage observed for myoglobin adsorbing to Ni(II)-DSIDA is consistent with binding by either His-48 or His-81 in a nearly end-on orientation. No multiple histidine combination is consistent with the observed thickness at low coverage if the protein retains its native conformation. The slight increase in thickness with coverage could indicate reorientation from a slightly tilted to a purely end-on orientation. This degree of reorientation could occur without a change in the binding site. We note that a few possibilities exist for binding by two sites that are consistent with the observed thickness but require small conformational changes to occur, such as binding by His 81 and His 82 or binding by His 116 and His 119.

The thinner dimension observed at low coverages for myoglobin adsorbing to Cu(II)-DSIDA is consistent with either partial denaturation or a side-on orientation. The latter would occur for binding by some combination of His-36, His-113, and His-116. However, a side-on orientation would result in a constant thickness of ∼25 Å independent of coverage. The increase in thickness with coverage in the case of Cu(II)-DSIDA indicates that simple side-on adsorption is not a sufficient explanation. There appear to be two possible explanations. First, upon completion of a monolayer, crowding could cause the molecules to tilt to an end-on orientation to allow more molecules to adsorb. In this scenario, no further increase in segment volume fraction would occur after completion of a monolayer in side-on orientation, as the molecules would simply tilt. This interpretation is illustrated in Figure 8, and the expected trends for the thickness and averaged segment volume fraction are given in Figure 9. The preference for a side-on orientation in the case of

(76) The importance of His-113 and His-116 for binding was examined in a study comparing the affinity of sperm whale myoglobin and dog myoglobin to chromatographic columns functionalized with Co(II)-IDA and Zn(II)-IDA.[13, 77] Sperm whale and dog myoglobin differ only by the fact that His-113 and His-116 are present in sperm whale myoglobin but absent in dog myoglobin. Sperm whale myoglobin was shown to have much greater affinity for chromatographic columns functionalized with Co(II)-IDA and Zn(II)-IDA than did dog myoglobin.[13, 77] A similar result was reported comparing horse and human myoglobins, where horse myoglobin showed a much greater affinity for Co(II)-IDA and Zn(II)-IDA than did human myogobin. His-113 and His-116 are present in horse myogobin but absent in human myoglobin. The interaction energy of histidine with Co(II)-IDA is comparable to that with Zn(II)-IDA. Both are weaker than the interaction of histidine with Ni(II)-IDA.[1] The authors concluded that the close spatial location of these two histidines was particularly important in binding to M(II)-IDA. However, in a later study by another group, no enhanced affinity (relative to that when the two histidines are separated over a larger distance) for Cu(II)-IDA was observed when a similar His-X2-His sequence was engineered into a surface helix in bovine stromatotrophin.[1, 78] This group went on to argue that His-X3-His is the optimal sequence on an α-helix that leads to enhanced binding.[79] They concluded that the enhanced binding in the earlier study was due to the multiplicity of sites rather than an optimal spatial distribution on the α-helical sequence for binding. Indeed, Arnold has shown a fairly strong correlation of apparent binding constant with multiplicity of surface exposed histidines on various proteins, regardless of their positioning.[1,0] This is consistent with a nonequilibrium process, in that multiple sites would increase the probability of an interaction occurring with the correct orientation for binding regardless of spatial distribution. For an equilibrated system, enhanced affinity would occur when multiple sites bound simultaneously, and therefore spatial distribution would be critical.

(77) Sulkowski, E. *Trends Biotechnol.* **1985**, *3*, 1.

(78) Suh, S.-S. Arnold, F. H. *Biotech. Bioeng.* **1990**, *35*, 682.

(79) Du, Y. Z.; Saavedra, S. S. *Langmuir* **2003**, *19*, 6443.

(80) We refer to the binding constants as "apparent" because we believe that the systems are not at equilibrium.

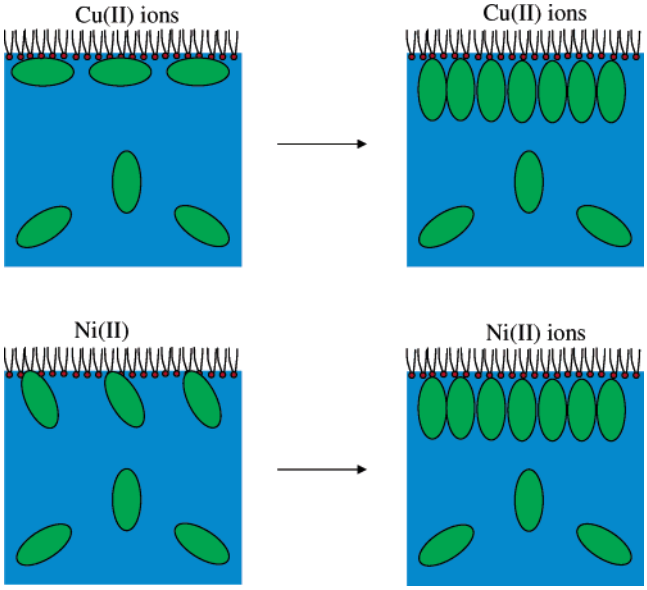

Figure 8. Schematic illustration of the interpretation based on different preferred orientations for isolated adsorbed myoglobin molecules for Cu(II)- and Ni(II)-loaded DSIDA. (a) Myoglobin adsorbs side-on to Cu-loaded DSIDA but tilts at high packing density to an end-on orientation. (b) Myoglobin adsorbs end-on to Ni(II)-loaded DSIDA.

Cu(II) but an end-on orientation for Ni(II) could be explained by the stronger interaction energy overcoming the greater entropic penalty for a side-on orientation and/or perhaps a slight strain of the structure to achieve multiple-site binding. However, an important difficulty with this interpretation is that the location of binding would have to change from His-36, His-113, and His-116 to either His-48 or His-81 in order to change from a side-on to an end-on orientation. This seems to conflict with the observation that adsorption is irreversible on our experimental time scale, although we note that one previous study reported reorientation for a system that was irreversible with respect to bulk concentation.[38] Another problem with this interpretation is that, whereas the initial thickness is lower for Cu(II)-DSIDA and the initial slope of the segment volume fraction versus surface density is stronger for Cu(II)-DSIDA, the results in Figure 4a and b do not strictly follow the expectations for this interpretation in Figure 9. Rather, the thickness is observed to increase nearly linearly for the entire adsorption process and the segment volume fraction does not level off prior to completion of adsorption.

An alternative interpretation that we believe to be more strongly supported by the data is that the conformation of isolated myoglobin molecules is altered somewhat upon adsorption to Cu(II)-DSIDA. In contrast to denaturation in bulk solution, which results in unfolding to a more open structure, surface denaturation can lead to spreading of a protein at a surface.[52,61,62] Surface denaturation is thus consistent with a thinner dimension for the adsorbed layer. The increase in layer thickness with coverage could arise from additional protein molecules adsorbing and partially denaturing until the surface sites are all occupied or blocked, as illustrated in Figure 10. This interpretation seems to be more consistent with the trends in thickness and segment volume fraction with adsorbed amount in Figure 4. The strong interaction energy of histidine with Cu(II)-DSIDA could result in distortions of the conformation upon adsorption to allow an increased number of histidine/Cu(II)-IDA interactions, including possibly those histidine residues that are buried within the structure in

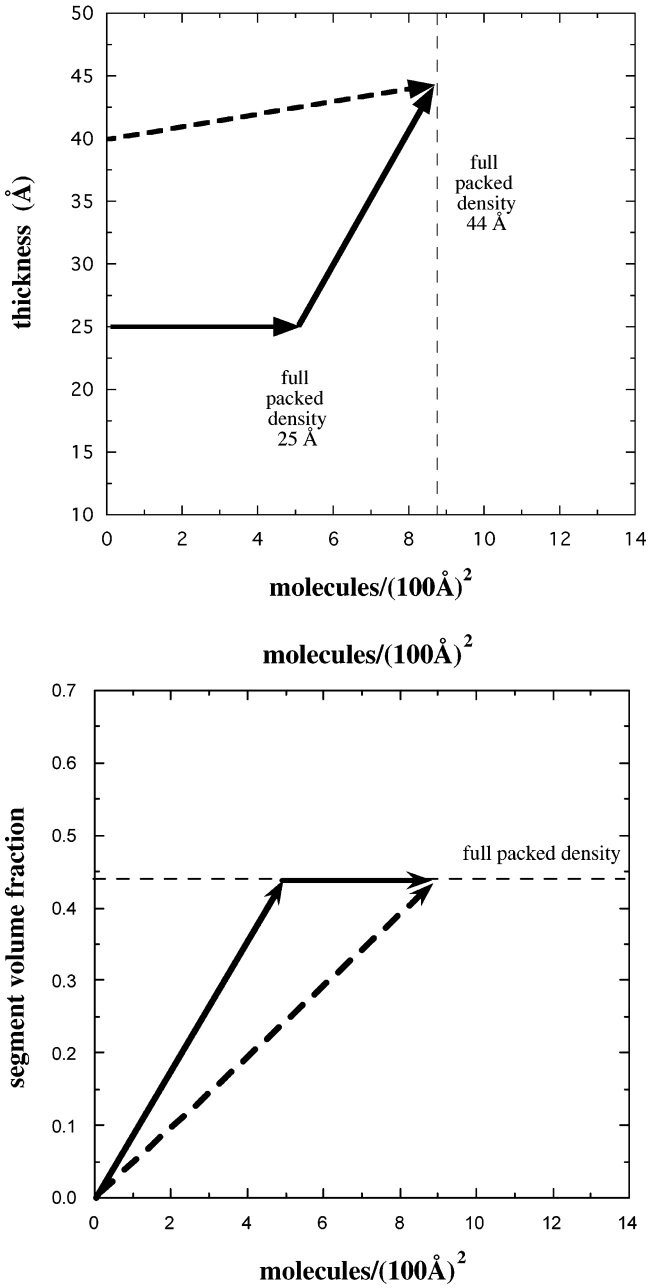

Figure 9. (a) Expected change in layer thickness versus coverage corresponding to the illustration in Figure 8: Cu(II) ions (solid lines), Ni(II) ions (dashed line). (b) Expected change in segment volume fraction versus coverage corresponding to the illustration in Figure 8: Cu(II) ions (solid lines), Ni(II) ions (dashed line).

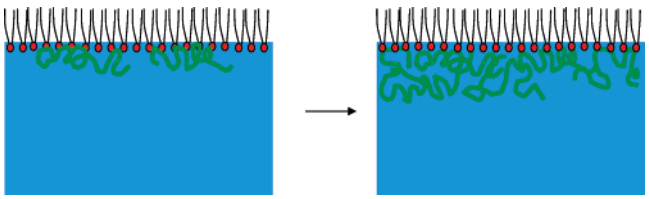

Figure 10. Schematic illustration of the adsorption process when partial denaturation occurs.

the native state. The relatively large interaction energy of 8.4kT for histidine/(Cu(II)-DSIDA can explain why a number of substantially weaker interactions (hydrogen bonds of order 1 kcal/mol or 1−2kT and hydrophobic and electrostatic interactions) supporting the secondary or tertiary structure of myoglobin could be compromised to

enable additional histidine/Cu(II)-IDA interaction sites. The weaker interaction energy for histidine/Ni(II)-IDA would result in less alteration of secondary or tertiary structure. The surface pressure data in Figure 6 provide further support for the interpretation of the differences in the structural data based on conformational changes rather than reorientation.

Finally, analogous experiments conducted with lysozyme, to be reported in detail elsewhere, provide additional insight that bears on the interpretation of the myoglobin adsorption data. Lysozyme has only one histidine, which is located on the exposed surface. Strong adsorption of lysozyme to DSIDA loaded with either Ni(II) or Cu(II) was observed. Moreover, adsorption was irreversible upon dilution of the subphase for either metal ion even at early stages of adsorption. This result indicates that binding by a single histidine to either bound metal ion is irreversible. The lysozyme results thus provide further support for interpretation of the data in Figure 4 in terms of conformational changes rather than reorientation.

Future work may provide more stringent tests of the above interpretations. Polarized fluorescence measurements have been shown to yield the mean tilt angle of the heme group and the breadth of the distribution.[53,54] A preferred orientation and retention of the native conformation would yield a narrow distribution of the tilt angle, whereas extensive conformational changes upon adsorption would presumably yield a broad distribution of the tilt angle.[76]

In both cases, the segment volume fractions at the later stages of adsorption exceed that calculated for myoglobin in the crystalline state. This seems to indicate that some denaturation may occur in both cases for densely packed layers, or perhaps the hydration state of adsorbed myoglobin is different from that for crystals formed in bulk solution.

V. Summary

This work presents a new level of detail regarding the structure of proteins adsorbing to lipid films through specific interactions using time-resolved neutron reflection. Measuring the change in structural characteristics versus time provides distinctive trends that can reveal subtle differences in the nature of the adsorption process. The data have revealed differences for myoglobin adsorbing to Cu(II)-DSIDA and Ni(II)-DSIDA. Distinct differences were observed in the evolution of the thickness and in-plane averaged segment density of the layer as a function of the areal density of molecules adsorbed. These differences are due to different interaction strengths in the two cases combined with the existence of multiple potential binding sites (histidines). The adsorbed layer at low coverage had a reduced thickness in the case of adsorption to Cu(II)-DSIDA relative to that for adsorption to Ni(II)-DSIDA. The layer characteristics were similar at full coverage. The structural characteristics at a given low surface density were the same whether obtained for low bulk myoglobin concentrations at long times or at high bulk concentrations at short times. The results appear to indicate that isolated myoglobin molecules denature to a greater extent upon adsorption to Cu(II)-loaded DSIDA than to Ni(II)-loaded DSIDA. More extensive denaturation in the case of binding to Cu(II)-DSIDA can be explained by the larger interaction energy.

The adsorption process was shown to be irreversible with respect to bulk concentration on a time scale of 8 h even at low coverages for both chelated metal ions. The time scale for adsorption in the present case is much slower than has been commonly observed for adsorption of proteins to hydrophobic or hydrophilic surfaces by nonspecific interactions. This may be due to a requirement of precise positioning for binding to occur.

Acknowledgment. Sandia is a multiprogram laboratory operated by Sandia Corporation, a Lockheed Martin Company, for the United States Department of Energy under Contract No. DE-AC04-94AL85000. This work has benefited from the use of the Los Alamos Neutron Science Center at the Los Alamos National Laboratory. This facility is funded by the U.S. Department of Energy under Contract No. W-7405-ENG-36. We also acknowledge the support of the National Institute of Standards and Technology, U.S. Department of Commerce, in providing neutron research facilities for this work.

LA047433Q